Mechanics of Composite Materials, Vol. 45, No. 5, 2009

THE EFFECT OF PRETENSIONED FRP WINDINGS ON THE BEHAVIOR OF CONCRETE COLUMNS IN AXIAL COMPRESSION

E. Zīle,[*] M. Daugevičius,[**] and V. Tamužs[*]

Keywords: *confined concrete, pretension, knee point*

This paper presents the results of an experimental investigation of concrete columns confined by wound pretensioned epoxy-impregnated carbon filament yarns. The yarn winding equipment, with the ability to set the desired pretension force and thereby to produce confined concrete specimens with different initial lateral pressure, was developed at the Institute of Polymer Mechanics. It is shown that the pressure increases the axial stress at which intense internal cracking of concrete develops.

Introduction

During the last decade, more and more research efforts have been focused on the use of CFRPs (carbon-fiber-reinforced plastics) as a reinforcement for concrete elements. The deterioration of old structures, the need for strengthened structural members because of increased loads, and the rehabilitation of existing structures (especially in highly seismic regions) are some of the applications where the CFRP reinforcement can be efficiently utilized.

In particular, CFRPs can be used to confine the lateral deformation of concrete columns subjected to axial compressive loadings. Confined concrete possesses a greatly enhanced strength and ultimate strain [1]. CFRP is linearly elastic up to failure, and when used as a confinement, it creates an ever-increasing lateral confining pressure on the concrete. As a result, a triaxial compressive stress state is created in it. The axial stress–axial strain curves of the confined concrete can be roughly considered bilinear. The first part of the curve corresponds to undamaged concrete. When the transition point, or knee point, is reached, intense internal cracking of the concrete begins. Due to the confinement, concrete does not fail, and the curve continues as a straight line with a greatly reduced slope.

The axial stress at the knee point is considerably higher if the column contains a longitudinal steel bar reinforcement [2]. This effect is caused by redistribution of the axial stress between the concrete and reinforcing bars, which lowers the stress level in concrete.

The knee point can be raised by laterally pretensioning the confining element, so that there arises an initial lateral stress acting on the column. One of the ways to achieve this is the chemical pretensioning [3]. In this method, a preformed con-

*Institute of Polymer Mechanics, University of Latvia, Aizkraukles St. 23, Riga, LV-1006, Latvia. **Department of Reinforced Concrete and Masonry Structures, Vilnius Gediminas Technical University Sauletekio Al. 11, 10223 Vilnius, Lithuania. Russian translation published in Mekhanika Kompozitnykh Materialov, Vol. 45, No. 5, pp. 663-676, September-October, 2009. Original article submitted May 14, 2009.

0191-5665/09/4505-0457

TABLE 1. Concrete Properties

Concrete target strength, MPa	Compressive column strength f_{co}, MPa	Ultimate axial strain $_{co}$, %	Ultimate lateral strain $_{l_0}$, %	Young's modulus E_b, GPa	Poisson ratio
20	18.7	0.30	0.16	24.1	0.21
35	38.1	0.26	0.15	29.7	0.20
50	44.6	0.24	0.10	32.6	0.20

TABLE 2. Split-Disk Test Results

Number of layers	Cross-sectional area of the composite, mm^2	Strength of the composite, MPa	Tensile modulus of the composite, GPa	Ultimate strain, %
2	12.04	513	37.2	1.14
4	15.61	901	57.2	1.30

fining tube (jacket) is placed around an existing concrete column, and then a mix comprising cement, sand, and an expansive agent is inserted between the concrete column and the jacket. The jacket confines expansion of the grout during the hardening period, and thus a chemical pretensioning occurs in the jacket, reacting against the concrete core.

The main objective of this work is to study the mechanical behavior of confined concrete columns if the confinement is created by winding initially pretensioned carbon filament yarns onto a rotating concrete specimen.

1. Experimental Program

1.1. Concrete properties. The compressive behavior of concrete of three different target compressive strengths (20, 35, and 50 MPa) were investigated on specimens in the form of cylindrical columns. The concrete was prepared in laboratory and was allowed to harden in forms under ambient conditions for 28 days. Six unconfined plain concrete columns were tested in a monotonic compressive loading to estimate their compressive strength. The diameter of all columns (both confined and unconfined) was 152 mm and length 300 mm. During the tests, axial and lateral strains were measured by strain gages glued at the column midheight. The results are summarized in Table 1.

1.2. Composite confinement properties. The concrete specimens were confined by winding a carbon yarn, impregnated with epoxy resin, tangentially around them. The yarn was a collection of parallel continuous carbon filaments.

Properties of the Tenax-J UTS 7731 carbon yarn (manufacturer's data): tensile strength 5193 MPa, tensile modulus 244 GPa, elongation at break 2.13%, density 1.79 g/cm^3, filament diameter 7 m, number of filaments 24,000, and cross-sectional area of the yarn 92.4 10^{-2} mm^2.

Such data are usually exaggerated and therefore cannot be used directly for estimating the strength of a composite. Therefore, split-disk tests according to the ASTM D 2290 standard were performed to determine the hoop properties of the composite jacket created. Two types of ring-shaped specimens (with two and four yarn layers) were prepared with a diameter of 157 mm and overlap length of 120 mm. All the rings were tested at a displacement rate of 2 mm/min up to failure. The results obtained are summarized in Table 2. A comparison of the experimental strength and modulus of the carbon yarn, calculated by the simple rule of mixtures (neglecting the strength and modulus of matrix), with manufacturer's data is shown in Table 3. It is seen that the values obtained for its elastic modulus, tensile strength, and ultimate tensile strain in the composite are by about 3, 33, and 43%, respectively, lower than the data given by the manufacturer.

1.3. Winding process and the confined specimens. Yarn winding is a technique for confining with a FRP, which consists in winding resin-coated fibers onto a rotating concrete specimen. The winding equipment used is shown in Fig. 1. A

TABLE 3. Experimental Values of Properties of the Tenax-JUTS7731 Carbon Yarn

Ratio between the cross-sectional areas of the yarns and the ring	Tensile strength, MPa			Young's modulus, MPa			Ultimate axial strain, %		
	Experiment	Average	Ratio between the average experimental and manufacturer's data	Experiment	Average	Ratio between the average experimental and manufacturer's data	Experiment	Average	Ratio between the average experimental and manufacturer's data
0.16	3206			233			1.14		
		3480	0.67		236	0.97		1.22	0.57
0.24	3754			238			1.30		

Fig. 1. Winding equipment: 1 — dynamometer; 2 — specimen; 3 — pretension device.

schematic diagram of the yarn winding process is depicted in Fig. 2. Continuous flow of the yarn is supplied from the bobbin to the pretension device. The pretension device is composed of four rubber-coated wheels. Each wheel is separately adjustable to obtain the pretension force desired. The placement of yarns was controlled by traversing the pretension device along the longitudinal axis of the specimen at a step of 8 mm per rotation. The resin was applied to the concrete surface and yarns before winding. The winding process was conducted carefully in order not to damage the yarns in the course of winding. The confined specimens were left to dry for a 10-day period at the temperature of 22 C.

Altogether, 26 confined specimens were tested in this study. The confining jacket consisted of two and four layers of wound yarns. The pretension force P of the yarn was equal to 0, 245, and 490 N. The axial and lateral strains were measured by both strain gages and linear variable displacement transducers (LVDT). The placement of the gages and LVDT is shown in Fig. 3. The loading rate was 10 MPa/min, following the ASTM C 39/C39M-99 standards.

2. Estimation of the Effect of Lateral Pretensioning of CFRP

It was shown in [4] that the increase in the compressive strength due to the confinement can be well estimated by the simple formula

$$\frac{f_{cc}}{f_{co}} \quad 1 \quad K \quad \frac{f_{lu}}{f_{co}}, \tag{1}$$

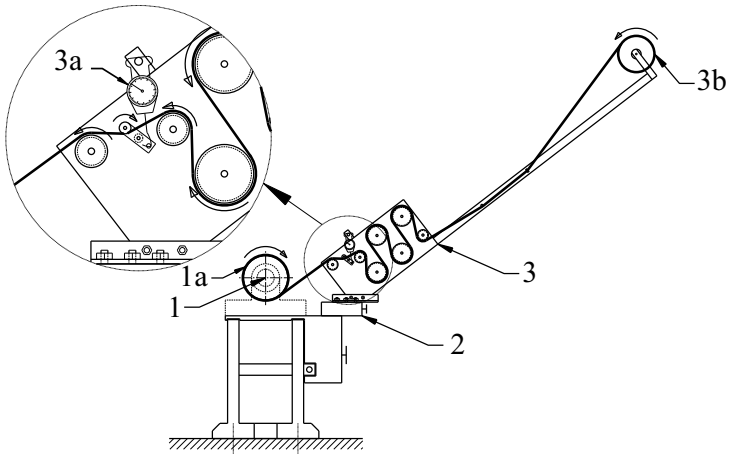

Fig. 2. Schematic diagram of the yarn winding equipment: 1— fixture of the rotating specimen; 1a — specimen; 2 — horizontal platform, moving along the longitudinal axis of the specimen; 3 — pretension device attached to the platform; 3a — dynamometer; 3b — yarn bobbin.

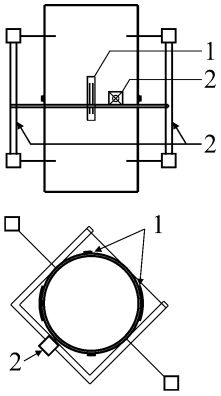

Fig. 3. Arrangement of strain gages (1) and LVDTs (2).

where f_{cc} is the confined concrete strength, f_{co} is the plain concrete strength, and f_{lu} is the ultimate lateral pressure. K is defined as

$$K \quad \frac{1}{\quad},$$

where is the initial Poisson ratio of concrete. For the typical value of the initial Poisson ratio 0.2, K = 4. The ultimate lateral pressure is expressed as

$$f_{lu} \quad \frac{E_j h}{R} \quad _{ju} \quad E_{lat} \quad _{ju},$$

where E_j is the elastic modulus of the CFRP jacket, h is the thickness of the jacket, R is the column radius, $_{ju}$ is the ultimate hoop strain of the jacket, and E_{lat} $E_j h/R$ is the so-called "lateral modulus". The ultimate lateral strain $_{lu}$ of the confined concrete is equal to the ultimate hoop strain of the jacket: $_{lu}$ $_{ju}$. If the jacket is made from a wound yarn, its thickness is

$$h \quad \frac{nS_0}{t},$$

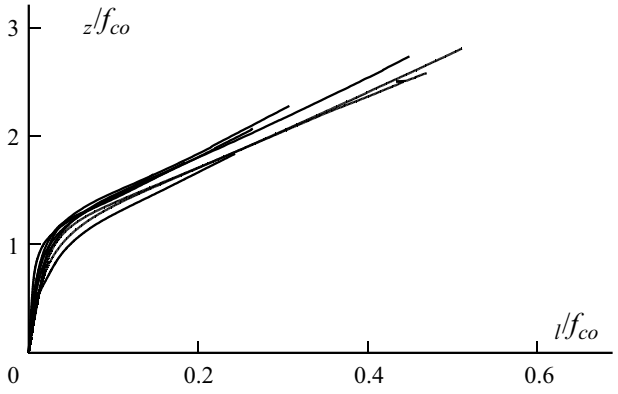

Fig. 4. Loading paths of confined concrete specimens [5].

where S_0 is the average cross-sectional area of the yarn, t is the winding pitch of the yarn, and n is the number of yarn layers.

It can be shown that, assuming Hook's law for concrete, the slope of the initial loading path in the stress space is

$$\frac{d \quad z}{d \quad l} \quad \frac{1 \quad k(1 \quad)}{k}, \tag{2}$$

where $\quad z$ is the axial stress, $\quad l$ is the lateral stress, and k is a parameter that characterizes the stiffness of the jacket:

$$k \quad \frac{E_j h}{E_b R},$$

where E_b is the initial elastic modulus of plain concrete.

When the initial loading path reaches the strength line [Eq. (1)], intense internal cracking of concrete starts. However, the confining jacket acts in such a way that the concrete column does not fail, but the loading path bends and becomes roughly parallel to the strength line. The failure of concrete occurs when the hoop stress in the composite jacket reaches its ultimate value. The intersection point of the initial loading path and the strength line is called the knee point or the limit of linearity. An example of loading paths in the axes of nondimensional normalized axial stress $\quad z$ and normalized lateral stress $\quad l$ for specimens with different plain concrete strengths and different confinement thicknesses is shown in Fig. 4 [5]. It is remarkable that all the loading paths follow a single master curve, which can be described by

$$\frac{| \quad z|}{f_{co}} \quad 1 \quad K \quad \frac{| \quad l|}{f_{co}}. \tag{3}$$

From Eq. (2) it follows that the lateral stress in the elastic regime is

$$l \quad \frac{k}{1 \quad k(1 \quad)} \quad z. \tag{4}$$

Insertion of Eq. (4) into Eq. (3) leads to the expression for the axial stress at the knee point

$$| \quad z| \quad [1 \quad k(1 \quad)] f_{co}. \tag{5}$$

This stress $| \quad z|$ can be increased by laterally pretensioning the CFRP jacket. The pretensioning creates an initial lateral stress $\quad l_0$, therefore, the initial loading path will intersect the strength line at a higher axial stress (Fig. 5). The initial lateral stress can be written as

$$l_0 \quad \frac{nP}{Rt},$$

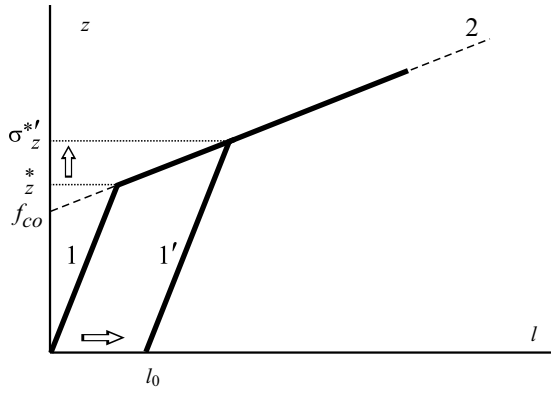

Fig. 5. Schematic representation of the influence of lateral stress on the knee point: 1 — loading of nonpretensioned specimens; 1 — loading path of pretensioned specimens; 2 — the strength line.

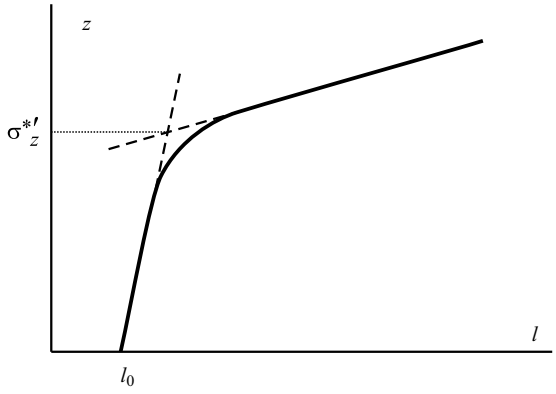

Fig. 6. Determination of the knee point from experimental data.

where P is the pretension force applied to the yarn. Now, the lateral stress in the elastic region is

$$l \quad \frac{k}{1 \quad k(1 \quad)} \quad z \qquad l_0 . \tag{6}$$

Insertion of Eq. (5) into Eq. (3) leads to the expression for the axial stress at the knee point in prestressed concrete

$$| \quad _z | \quad [1 \quad k(1 \quad)][f_{co} \quad K \quad | \quad _{l_0} |]$$

or

$$| \quad _z | \quad [1 \quad k(1 \quad)] \; f_{co} \quad \frac{1}{} \quad \frac{nP}{Rt} \quad . \tag{7}$$

In reality, there is no sharp transition from the first to the second part of the loading path, therefore, the knee point is defined as the axial stress at the intersection of continuations of linear sections of the first and second parts of the paths (Fig. 6).

3. Results

The averaged stress–strain curves – of the confined concrete specimens are shown in Fig. 7. The loading paths in the normalized stress space are depicted in Fig. 8. Table 4 lists the experimental characteristics of confined and unconfined con-

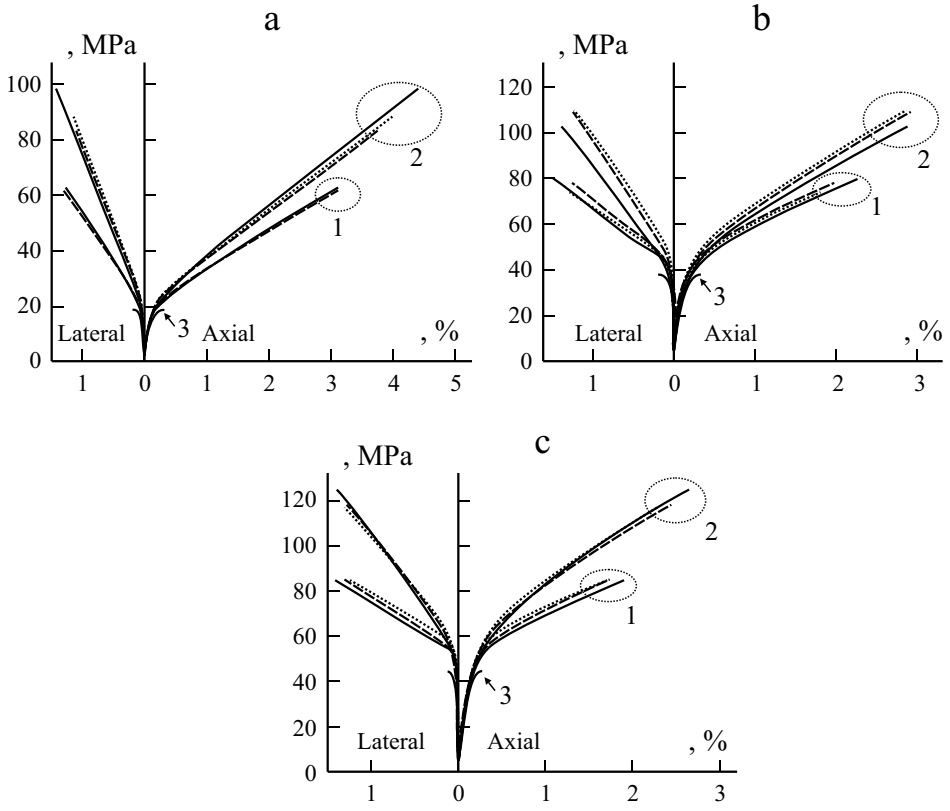

Fig. 7. Stress–strain curves – of columns with 2 (1) and 4 (2) layers at $P = 0$ (——), 245 (- - -), and 490 N ( ). The strength of the unwrapped columns (3) f_{co} = 18.7 (a), 38.1 (b), and 44.6 MPa (c).

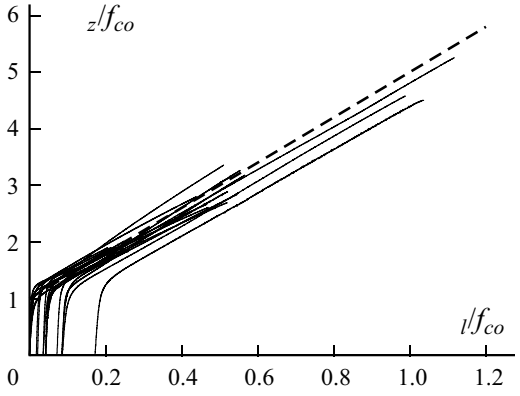

Fig. 8. Loading paths in the present study: (- - -) — the strength line.

crete specimens. The relative increment of the axial stress at the knee point due to the initial prestress, , is calculated as follows:

$$\frac{|\ _z|\ -\ |\ _z|}{|\ _z|}\ 100\%. \tag{8}$$

The estimated relative increment ^{est} is obtained by inserting Eqs. (5) and (7) into Eq. (8):

TABLE 4. Experimental Results

f_{co}, MPa	n	P, N	$\lvert_0\rvert$, MPa	$_{cc}$, %	$_{lu}$, %	f_{cc}/f_{co}	$\lvert_z\rvert^{exp}/f_{co}$	$\lvert_z\rvert^{est}/f_{co}$
18.7	2	0	0	3.15	1.29	3.36	1.04	1.02
		245	0.81	3.15	1.33	3.31	1.08	1.20
		490	1.61	2.99	1.23	3.21	1.16	1.38
18.7	4	0	0	4.39	1.41	5.26	1.00	1.05
		245	1.61	3.74	1.09	4.45	1.11	1.41
		490	3.22	4.08	1.17	4.74	1.24	1.77
38.1	2	0	0	2.28	1.50	2.10	1.06	1.02
		245	0.81	1.96	1.26	2.05	1.16	1.10
		490	1.61	1.82	1.28	1.94	1.16	1.19
38.1	4	0	0	2.88	1.39	2.70	1.05	1.04
		245	1.61	2.91	1.23	2.89	1.16	1.21
		490	3.22	2.90	1.23	2.88	1.27	1.39
44.6	2	0	0	1.91	1.41	1.90	1.19	1.02
		245	0.81	1.73	1.30	1.90	1.24	1.09
		490	1.61	1.76	1.26	1.91	1.29	1.17
44.6	4	0	0	2.66	1.38	2.80	1.24	1.04
		245	1.61	2.49	1.30	2.67	1.29	1.19
		490	3.22	2.28	1.28	2.61	1.40	1.34

Note: $_{cc}$ and $_{lu}$ are the average ultimate axial and lateral strains, respectively, of confined specimens; f_{cc}/f_{co} is the normalized compressive strength of confined specimens; $\lvert_z\rvert^{exp}/f_{co}$ is normalized axial stress at the knee point for confined specimens; $\lvert_z\rvert^{est}/f_{co}$ is the estimated normalized axial stress at the knee point.

$$_{est} \quad \frac{1}{} \quad \frac{nP}{Rt}.$$

The experimental and estimated relative increments of axial stress at the knee point due to the initial prestress, for all the confined specimen configurations tested, is shown in Fig. 9.

4. Discussion

It is seen form Fig. 9 that the pretensioning of CFRP can increase the knee point by up to 24%. According to [6], the compressive stresses in a plain structural concrete element should not exceed the limiting one:

$$_z \quad 0.6\frac{f_{co}}{},$$

where is the safety factor (1). For confined structural elements, f_{co} is replaced by the knee point $\lvert_z\rvert$. In most cases, $\lvert_z\rvert$ f_{co} for nonprestressed confined elements. Since $\lvert_z\rvert$ f_{co} for prestressed structural elements, they have higher limiting stresses and can be subjected to higher service loads.

There is a significant difference between the estimated and experimental increments of the knee point for some of the configurations tested (Fig. 9). This indicates that the prestress level achieved was much lower than intended. This can be explained by a possible stress relaxation and creep in the confined specimens during the drying period, which reduced the prestress level. This effect is especially pronounced for the low-strength concrete (f_{co} = 18.7 MPa).

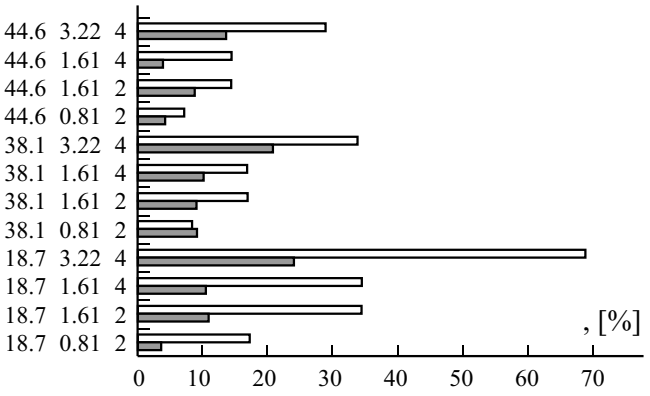

Fig. 9. Experimental (■) and estimated (□) relative increments of the axial stress at the knee point due to the initial prestress. The following labeling of confined specimens is used: plain concrete strength [MPa] — initial prestress [MPa] — L (number of confinement layers).

TABLE 5. Estimated Relative Increase in the Compressive Strength due to the Yarn Winding Technique

f_{co}, MPa	E_{lat}, MPa	$(f_{cc}$ $f_{cc})/f_{cc}$, %
27	1170	37
27	2730	50
48	1170	28
48	2730	42

The drawback of the initial pretension of CFRP is a reduction in the deformation capacity of the composite jacket, because it contains already prestretched yarns. It is seen from Fig. 9 that most of the prestressed confined specimens have a lower ultimate lateral strain than those without an initial prestress. The lowered deformation capacity of CFRP leads to a lower strength and a lower ultimate axial strain. However, this is of no importance in practical applications, because the service load of structural concrete elements is lower than the knee point.

The compressive strength depends on the ultimate hoop strain of the CFRP jacket [see Eq. (1)]. It is found in [1, 5] that the ultimate CFRP hoop strain in confined concrete tests is about 40% lower than that in the split-disk test if the concrete is confined manually by winding a continuous carbon yarn tape impregnated with epoxy resin around a column, with yarns oriented in the hoop direction. Tests show that, for concrete confined by a wound carbon yarn, the ultimate hoop strain is about the same or even higher than that obtained from the split-disk test. This means that yarn winding produces a more qualitative confinement by providing a better fiber distribution and minimizing the fiber waviness. From two specimens having the same plain concrete strength and lateral modulus, the specimen with a prestressed jacket will have a higher compressive strength than that wrapped manually. If f_{cc} and $_{ju}$ are the compressive strength and ultimate hoop strain of the manually wrapped concrete column ($_{ju}$ 0.6 $^{d}_{ju}$, where $^{d}_{ju}$ is ultimate hoop strain in the split disk test), and f_{cc} is the compressive strength of the concrete column with a prestressed winding, then, according to Eq. (1), the relative increase in the compressive strength due to the prestressed winding can be roughly estimated by the formula

$$\frac{f_{cc} \quad f_{cc}}{f_{cc}} \quad \frac{0.67K \quad E_{lat} \quad _{ju}}{f_{co} \quad K \quad E_{lat} \quad _{ju}}.$$

The relative increase in the compressive strength is greater for the concrete of lower strength. As reported in [5], ε_{ju}^{d} = 1.2% and E_j = 225,000 MPa for the CFRP. The estimated relative increase in the compressive strength due to the pretensioned yarn winding, for some of the specimens tested in [5], is reported in Table 5.

Conclusions

The pretensioning of CFRP creates an initial later stress which delays the start of intense internal cracking of confined concrete.

The pretensioning increases the axial stress at the knee point by up to 24% compared with that without pretensioning. This means that laterally prestressed structural concrete elements can be subjected to higher service loads than nonprestressed ones.

To fully utilize the deformation capacity of CFRP yarns, winding is recommended instead of manual wrapping of a resin-impregnated tape around the column. For the same plain concrete strength and lateral modulus, the specimen with a prestressed jacket will have a higher compressive strength than the manually wrapped one (Table 5).

Acknowledgments. The authors would like to thank Mr. J. Silis (Institute of Polymer Mechanics) for making the winding equipment.

REFERENCES

1. V. Tamuzs, R. Tepfers, Chi-Sang You, T. Rousakis, I. Repelis, V. Skruls, and U. Vilks, "Behavior of concrete cylinders confined by carbon-composite tapes and prestressed yarns. 1. Experimental data," Mech. Compos. Mater., **4**2, No. 1, 13-32 (2006).
2. V. Tamuzs, V. Valdmanis, K. Gylltoft, and R. Tepfers. "Behavior of CFRP-confined concrete cylinders with a compressive steel reinforcement," Mech. Compos. Mater., **43**, No. 3, 191-202 (2007).
3. A. A. Mortazavi, K. Pilakoutas, and Ki Sang Son. "RC column strengthening by lateral pre-tensioning of FRP," Constr. Build. Mater., **17**, 491-497 (2003).
4. V. Tamuzs, R. Tepfers, and E. Sparnins, "Behavior of concrete cylinders confined by a carbon composite. 2. Prediction of strength," Mech. Compos. Mater., **42**, No. 2, 109-118 (2006).
5. V. Tamuzs, R. Tepfers, E. Zile, and O. Ladnova. "Behavior of concrete cylinders confined by a carbon composite 3. Deformability and the ultimate axial strain," Mech. Compos. Mater., **42**, No. 4, 303-314 (2006).
6. Comité Euro-International du Beton. CEB-FIP Model Code 1990. Bulletin d'Information CEB, 213/214, Lausanne (1993).